2005

Absolute wave-number measurements in 130Te2: Reference lines spanning the 420.9-464.6-nm region

T.J. Scholl

Steven J. Rehse
University of Windsor

R.A. Holt

S.D. Rosner

Absolute wave-number measurements in $^{130}Te_2$: reference lines spanning the 420.9–464.6-nm region

T. J. Scholl, S. J. Rehse, R. A. Holt, and S. D. Rosner

Department of Physics and Astronomy, University of Western Ontario, London, Ontario, Canada N6A 3K7

Received September 23, 2004; revised manuscript received December 6, 2004; accepted December 13, 2004

We have measured the absolute wave numbers of 39 transitions of $^{130}Te_2$ spanning the spectral region of 420.9–464.6 nm to an accuracy of better than 2 parts in 10^9 by use of saturation spectroscopy and Fabry–Pérot interferometry. These measurements provide a set of convenient and accurate transfer standards for laser wavelength calibration spanning the entire Stilbene-420 dye-tuning curve. © 2005 Optical Society of America

OCIS codes: 300.6360, 300.6460, 300.6550, 300.6320, 120.2230, 120.3940.

1. INTRODUCTION

Molecular absorptions are convenient absolute standards for the wavelength measurement of laser sources used for spectroscopy and optical fiber telecommunications. The characterization of wavelength-division-multiplexing components and the calibration of test equipment for telecommunications require absolute wavelength measurements based on absorptions in simple molecules such as HF, acetylene, HCN, and CO.[1–5] Extensive atlases of molecular absorption lines in I_2,[6–8] Br_2,[9] and Te_2[10,11] that span much of the visible and near-infrared regions of the spectrum have been compiled with Fourier transform spectroscopy. Typical accuracy for these Doppler-limited measurements is ~1 part in 10^7, which is sufficient for calibration of broadband lasers and many spectra but falls short of the standards required for a precise wavelength determination of stabilized single-frequency lasers. A large number of Doppler-free measurements[12–18] of transition frequencies have been made for $^{127}I_2$. On the basis of systematic analyses of these and other Doppler-free measurements, extraction of molecular parameters for calculation of transition frequencies to better than a few parts in 10^9 has been possible.[16,19] Certain hyperfine splittings can be calculated with a precision of better than 30 kHz.[17]

With the exceptions of the Los Alamos Th and U emission atlases,[20,21] the Te_2 atlas is the only convenient set of wavelength references available for wavelengths of less than 500 nm. The accuracy of the emission atlases, ~0.003 cm^{-1}, is similar to that of Te_2; however, the density of measured lines is much smaller. The number of high-precision Doppler-free studies of $^{130}Te_2$ is small in comparison with $^{127}I_2$, probably owing to the increased difficulty in producing tunable single-frequency light in this spectral region. Several experimenters[22–26] have concentrated on transitions in the vicinity of 486 and 488 nm for use as references in precision measurements of hydrogenic atoms (deuterium, hydrogen, positronium, and muonium) with typical accuracies exceeding 1 part in 10^9. In addition to these measurements, Courteille *et al.*[27] measured the wave numbers of 18 transitions near 467 nm to an accuracy of 2 parts in 10^8 for use as references in the precision spectroscopy of single trapped Yb^+ ions.

To establish standards over a broader wavelength range, Cancio and Bermejo[28] measured 16 transitions from 476 to 529 nm with an accuracy of approximately 1 part in 10^8. These wavelengths coincide with laser emissions from an argon ion laser and can be used for frequency locking. Further accurate determinations of transition wavelengths were made by Gillaspy and Sansonetti,[29] who measured the wave numbers of 32 selected transitions in the range of 471–502 nm spanning the tuning curve of the laser dye Coumarin 480. These transitions were measured with an accuracy of 2.2 parts in 10^9 and were confirmed by comparison with previous measurements. Gillaspy and Sansonetti noted that the atlas values for all of the transitions they measured were low by an average of 0.00204 cm^{-1}. Their conclusion was that the atlas values do not provide suitable wave numbers for Doppler-free transitions even if a constant offset is added, owing to the blending of several molecular lines into one line observed via Fourier spectroscopy.

No extended set of Doppler-free measurements of Te_2 transition wave numbers exists for wavelengths shorter than ~471 nm. With this in mind, we have measured the absolute wave number of 39 transitions in $^{130}Te_2$ from 420.9 to 464.6 nm with an accuracy of better than 2 parts in 10^9. These transitions are roughly equally spaced within this wavelength range and span the tuning curve of the laser dye Stilbene 420. Since we previously[30] compared the results of five transitions from 475.6 to 490.8 nm and found excellent agreement with previously established standards, these absorption lines should provide a useful set of new reference lines in this part of the optical

0740-3224/05/051128-6/$15.00

spectrum and eventually help form the basis of high-precision measurements for comprehensive theoretical modeling of the molecular spectrum.

2. APPARATUS AND METHOD

The details of the experimental apparatus, which is an improved version of one described by Sansonetti,[31] werepreviously published.[30] A schematic diagram of the apparatus is shown in Fig. 1. Tunable light for measuring the saturated absorption transitions in $^{130}Te_2$ is produced by pumping Stilbene 420 dye in a single-frequency cw dye laser with 4.5 W of UV light from an argon ion laser. Typical output powers range from ~75 to 300 mW across the dye-tuning curve. As shown in Fig. 1(a), light from the dye laser is split into a pump beam and a weaker probe beam and modulated by a dual-frequency chopper at 3000 and 2500 Hz, respectively. These beams are overlapped as they traverse a Te_2 cell in opposite directions. After the probe beam exits the cell, a portion of it is sampled by a beam splitter and is phase detected at the sum frequency (5500 Hz), producing an intermodulated saturation[32] spectrum. A typical Doppler-free line profile is shown in Fig. 2.

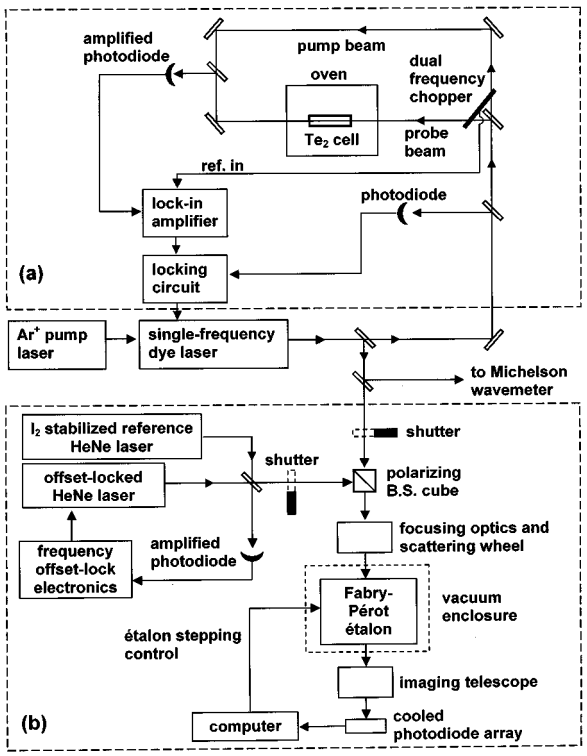

Fig. 1. Schematic apparatus diagram. (a) A major portion of the light from a single-frequency cw dye laser is split into separate pump and probe beams modulated by a dual-frequency chopping wheel and overlapped in a heated Te_2 cell. Feedback from the sum-frequency signal detected by a lock-in amplifier is used to lock the frequency of the dye laser to the saturated absorption signal. (b) The remaining dye laser light is directed to a Fabry–Pérot wavelength meter and to a Michelson wavelength meter (for coarse wavelength measurement). Light from the dye laser and a He–Ne laser offset locked to an I_2-stabilized He–Ne laser alternately illuminates the etalon, producing interference ring patterns on a photodiode array.

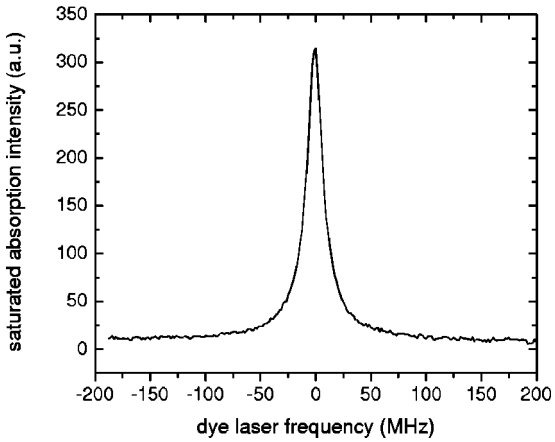

Fig. 2. Doppler-free saturated-absorption profile of the Te_2 line at 22 634 cm^{-1}. The linewidth (FWHM) is 17 MHz. The cell temperature was 502°C corresponding to a vapor pressure of 91 Pa, and the pump beam and probe beam powers were approximately 100 mW and 10 mW, respectively.

A 7.5-cm long, 2.5-cm-diameter quartz $^{130}Te_2$ cell is heated in a tube furnace. The 502°C cold-finger temperature corresponds to a Te_2 vapor pressure of 91 Pa.[33] The temperature controller regulates the oven temperature to within 3°C, with an absolute accuracy of better than 2°C. We estimate that the total uncertainty of the cold-point temperature is ±6°C, including the uncertainty in the location of the coldest point on the finger. The cell body and windows are held at a temperature ~15–20°C warmer. The single-pass absorption through the Te_2 vapor at 502°C is 23(2)% for the Doppler-limited line at 20 564.385 cm^{-1}, in agreement with other work.[29] At the same cell temperature, the single-pass absorption at 22 634.330 cm^{-1} is 85(3)%.

The absolute wave number of the dye laser is measured by comparison with the wave number of a reference laser by use of an evacuated Fabry–Perot (FP) etalon, as shown in Fig. 1(b). Light from the dye laser and a He–Ne reference laser is expanded by lenses before being combined by a polarizing beam splitter. Computer-controlled shutters in the path of each laser beam select light from either laser, which is then focused by a 100-mm-focal-length cylinder lens to form a horizontal line source on a spinning plastic wheel. The exit side of the wheel is roughened to scatter the laser light and destroy its coherence, eliminating noise from laser speckle. The scattered light is collimated by an 80-mm-focal-length achromatic lens and masked by a 33-mm-diameter iris.

The etalon mirrors are aluminum coated with a reflectivity of 85% at 632.8 nm and a reflectivity finesse of 19.3. This low finesse is desirable in order to spread interference rings over several pixels of the photodiode array, allowing subpixel location of the maxima. Bare aluminum possesses excellent broadband reflectivity and optical phase shifts that vary smoothly with wavelength and are stable in time.[34,35] The entire etalon assembly is housed in a vacuum enclosure at a pressure less than 3.33 Pa. The assembly is constructed almost entirely from Super Invar (coefficient of linear expansion $\alpha \leq 0.36 \times 10^{-6}\,°C^{-1}$), with the exception of the alignment and scanning piezoelectric crystal transducers. The three

scanning piezoelectric transducers are used to systematically step the etalon spacing through a distance corresponding to a change of one interference order at the reference wavelength, providing an excellent check for systematic effects.[30] This represents an improvement over previous fixed-spacing FP-based wavelength meters, which are essentially static except for slow drifts in their mirror spacings.

The interference "ring" pattern of the etalon is projected by a 2000-mm-focal-length Schmidt–Cassegrain telescope onto a cooled EG&G Reticon 1024-element silicon linear photodiode array (PDA). The catadioptric telescope produces a more compact optical path and has far less chromatic aberration over a larger wavelength range than an ordinary refracting achromatic doublet. Residual background signal is eliminated by subtracting a pattern acquired with no light input. A single ring pattern is digitized in 13.5 ms, with typically 10 individual patterns averaged by the computer for analysis and display. A measurement cycle, which includes acquisition and analysis of 10 ring patterns for each laser, is completed in ~1 s.

The reference laser is a single-frequency 900-μW He–Ne laser that is frequency offset locked to a Winters Electro-Optics Model 100 He–Ne laser. The latter is stabilized to the *d* component of the R(127) 11-5 transition of $^{127}I_2$, whose frequency is known to a few parts in 10^{11}. The ~0.1 MHz uncertainty in the offset lock leads to an accuracy of $\sim 2 \times 10^{-10}$ for our reference wave number.

A dc ratio circuit is used to lock the dye laser frequency to the side of a given Te_2 saturated absorption line. Measurements of the laser wave number are made with the laser locked alternately to each side of the symmetric saturated-absorption lines and averaged. Typical observed line widths are 15–25 MHz. For strong absorption lines, power broadening of 5–7 MHz is observed at pump-beam powers greater than 50 mW. Variation of the lock points from 25 to 75% of maximum saturated absorption results in no statistically significant systematic shifts in the averaged line center.

The FP "ring" pattern is described by the Airy formula.[36] Each point can be assigned a (generally nonintegral) interference order number p. At the center of the pattern, p satisfies the relation

$$p \equiv P + \epsilon = 2t\sigma, \tag{1}$$

in which P is the integer part, ϵ is the fractional part, t is the mirror separation, and $\sigma = 1/\lambda$ is the wave number. The analysis of the FP ring patterns determines the fractional part of the interference order number at the center of the pattern for the unknown and reference wavelengths, ϵ and ϵ_{ref}, respectively.

An auxiliary traveling Michelson wavelength meter with a precision of better than 1 part in 10^7 is used to determine the integer parts of the order numbers. First we make a preliminary determination of the etalon spacing t using the method of exact fractions.[37] This requires a series of simultaneous measurements of the dye laser wave number σ and the fractional order ϵ spanning ~1000 cm^{-1}. Owing to the excellent length stability of the FP etalon this procedure is necessary only at the beginning of each day. Along with Eq. (1), this measurement of t is sufficient for calculation of the integer part of the order number for the standard laser, P_{ref}, from its known wave number, σ_{ref}. The exact value of p_{ref}, determined from P_{ref} and ϵ_{ref}, then yields a more accurate value of t. The Michelson wavelength meter is next used to make a preliminary measurement of the unknown wave number, from which we calculate the integer part P of its order number, again using Eq. (1) and t. The wave number σ of the Doppler-free Te_2 transition is then given by

$$\sigma = \frac{P + \epsilon}{P_{\mathrm{ref}} + \epsilon_{\mathrm{ref}}} \sigma_{\mathrm{ref}}. \tag{2}$$

A more precise condition for interference in the FP etalon includes a wave-number-dependent phase correction $\delta(\sigma)$ arising from reflection at the Al mirrors. This modifies Eq. (1) to be

$$P + \epsilon + \delta(\sigma) = 2t\sigma. \tag{3}$$

Here $\delta(\sigma_{\mathrm{ref}}) \equiv 0$, making it a relative correction. The true or phase-corrected wave number σ is related to the measured wave number σ_{meas} [determined from Eq. (2)] by

$$\sigma = \sigma_{\mathrm{meas}} + \frac{\delta(\sigma)}{2t}. \tag{4}$$

Phase corrections to the unknown wave number were previously measured[30] for the etalon mirrors used in this work by the method of virtual mirrors[38] for 10 wavelengths spanning the interval from 424.9 to 490.8 nm, which includes the narrower spectral region of this work (420.9–464.6 nm), except for 4.0 nm at the lower end. Since the physical origin of the phase shift[34,35] implies smooth behavior over this spectral region, a linear fit of $\delta(\sigma)$ versus σ, shown in Fig. 3, was used for interpolation.

As mentioned above in this section and detailed in Ref. 30, the ability to measure a wave number at different etalon spacings is an important check on possible sources of systematic errors. Accordingly, the frequency of the tunable dye laser is locked to the side of a saturated absorption feature, and its wave number is measured 50 times as the spacing of the FP etalon is stepped over one free spectral range of the etalon at σ_{ref}. When the wavelength

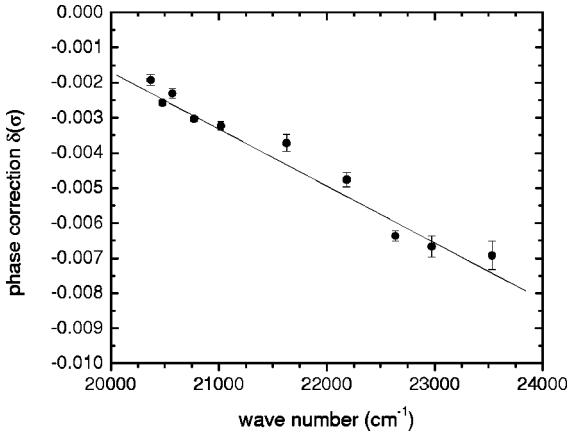

Fig. 3. Wave-number-dependent phase correction $\delta(\sigma)$ resulting from reflections at the FP etalon mirrors, measured previously[30] by use of the method of virtual mirrors for seven different spacings. The results for $\delta(\sigma)$ measured at 10 different wave numbers have been fitted to a straight line for interpolation.

Table 1. Measured Wave Numbers and Approximate Air Wavelengths for Doppler-Free Transitions in $^{130}Te_2$ at a Temperature of 502(6)°C Corresponding to a Vapor Pressure of 91(13) Pa.[a]

Wavelength (nm)	Wave Number (cm^{-1})	Wavelength (nm)	Wave Number (cm^{-1})
464.559	21 519.798 444(37)	439.475	22 748.075 796(37)
462.383	21 621.068 197(37)	439.473	22 748.169 719(37)
462.263[b]	21 626.668 960(37)	437.340	22 859.096 863(37)
461.507	21 662.099 758(37)	436.743	22 890.361 707(37)
459.450	21 759.054 591(37)	435.225[b]	22 970.191 921(37)
457.549	21 849.472 279(37)	433.874	23 041.730 708(37)
457.286	21 862.055 540(37)	433.866	23 042.161 281(37)
455.196	21 962.428 481(37)	433.103	23 082.724 412(37)
453.985	22 021.005 928(37)	431.517	23 167.540 846(37)
453.317	22 053.433 804(37)	431.014	23 194.587 007(37)
452.856	22 075.901 181(37)	428.952	23 306.123 768(37)
450.643[b]	22 184.304 882(37)	428.894	23 309.247 086(37)
449.571	22 237.195 680(37)	427.057	23 409.535 409(37)
448.317	22 299.386 951(37)	426.310	23 450.552 578(37)
448.317	22 299.399 264(37)	424.856[b]	23 530.779 797(37)
446.092	22 410.641 620(37)	424.160	23 569.392 054(37)
445.845	22 423.055 958(37)	422.801	23 645.177 731(37)
445.752	22 427.739 605(37)	421.674	23 708.323 012(37)
442.654	22 584.672 277(37)	420.883	23 752.932 043(37)
441.683[b]	22 634.330 275(37)		

[a]Uncertainties in wave numbers are one standard deviation.
[b]Lines used in the determination of the phase correction (see Fig. 3).

meter's optics are in optimum alignment, the standard deviation of these 50 measurements is typically less than 1 MHz. The dye laser is subsequently relocked to the opposite side of the absorption line and its wave number is measured in the same manner. The measured transition wave number is calculated as the average of these two measurements.

3. ANALYSIS

The FP pattern is analyzed by the usual "rings" method.[36] It can be shown from the Airy formula that, for light at near-normal incidence on the etalon, the radius r_j of the j_{th} ring satisfies

$$r_j^2 = s(j - 1 + \epsilon). \tag{5}$$

Therefore ϵ can be determined from a plot of r_j^2 versus j as $\epsilon = 1 + \text{intercept/slope}$. The individual ring radii are determined by the fitting of an approximation to the Airy function valid near a local maximum,[30] modified by a Gaussian envelope function (to correct for any distortions in the ring positions due to variations in the intensity envelope over a single ring).

Small distortions in the recorded ring pattern due to changes in the alignment of the etalon and the focusing of the ring pattern on the PDA can lead to errors in measuring ϵ. To monitor this effect, the data-acquisition program displays residuals for the plot of r_j^2 versus j, as well as the finesse of the pattern, in real time. Initially, the focus of the telescope is adjusted so that the residuals from this plot for ring patterns from both lasers can be minimized and randomized. The finesse of the etalon is subsequently maximized and the procedure iterated until no further improvement can be realized. So that the PDA is aligned along the horizontal diameter of the ring pattern, the telescope–PDA combination is translated in the vertical direction to maximize the observed value of ϵ. The position of the focused laser light on the scattering wheel is then reoptimized to produce a symmetric and maximized intensity distribution for the patterns. Finally, the telescope–PDA combination is translated until the optimized ring pattern is centered horizontally on the PDA.

Table 2. Systematic and Statistical Measurement Uncertainties (One Standard Deviation)

Source of Uncertainty	Uncertainty (MHz)
Residual gas dispersion	negligible
Reference frequency	negligible
Offset-lock frequency	0.20
Absorption line-shape asymmetry	0.20
Pump-probe parallelism	0.20
Pressure shifts	0.30
Phase correction	0.23
Repeatability of results (statistical)	0.97
Overall uncertainty (quadrature sum)	1.1

4. RESULTS

Our measured transition wave numbers for 39 saturated absorption lines are shown in Table 1, and a summary of our error budget is given in Table 2. Fifty repeated measurements of a given transition wave number over a span of a few minutes exhibit a submegahertz scatter. However, realignment of the wavelength meter optics produces small but noticeable shifts in the measured wave number and increases the longer-term measurement scat-

ter. This is probably due to minute changes in the alignment of the PDA relative to the center of the ring pattern and to distortions of the ring pattern due to changes of the optical alignment, including etalon finesse. The measurement reproducibility has therefore been estimated from the scatter of all transition wave-number measurements. From the weighted average for each transition wave number, the residuals for each individual measurement, acquired over several weeks, are compiled with those of all other transitions. A histogram of these residuals is shown in Fig. 4. The set of 457 measurements has 418 degrees of freedom, since these data are calculated from 39 measurement averages. The overall sample standard deviation of 0.97 MHz is taken as our estimate of the measurement reproducibility.

Another source of uncertainty comes from the phase correction δ obtained by interpolation in the linear fit shown in Fig. 3. The reduced χ^2 for this fit is 4.4, suggesting that the uncertainty in δ may be underestimated. A plausible reason for this is that each measurement of δ relies on a series of measurements of the wave number for a given transition at several different values of the etalon spacing t.[30] At small values of t, the value of σ is more sensitive to small changes in the focusing of the ring pattern onto the linear PDA because of residual chromatic aberration in the optics used for small t. It is important to note that measurements of σ at small t (which are inherently less accurate than at large t) were used *only* in the determination of δ, which is itself a small correction to σ. To account for the quality of the linear fit, we have chosen to set the uncertainty in the phase correction equal to the 3.4×10^{-4} rms residual of the fit. This is a more conservative estimate than one derived from the uncertainties of the fit parameters. The use of Eq. (4) to correct the transition wave numbers measured at a spacing of $\sim$22.5 cm in this experiment leads to an uncertainty in σ of $\pm 7.5 \times 10^{-6}$ cm^{-1} or 0.23 MHz.

Uncertainties in the wave numbers arising from residual gases in the FP vacuum and knowledge of the I_2-stabilized He–Ne frequency are negligible. The measurement uncertainty ($\sim$0.1 MHz) in the beat frequency used to offset lock the single-frequency He–Ne laser to the I_2-stabilized He–Ne laser leads to a wavelength meter uncertainty of 0.2 MHz for the spectral region of this work. The Te_2 cell vapor pressure is uncertain by a pressure of 13 Pa owing to the 6°C temperature uncertainty for the cell cold point. Typical pressure shifts for Doppler-free transitions in Te_2 vapor in this spectral region are $\sim$0.0075 MHz/Pa,[23–25] resulting in a pressure-shift uncertainty of 0.1 MHz. A conservative upper limit of 0.3 MHz for this systematic error is quoted, since the pressure shifts have not been measured for these transition wave numbers.

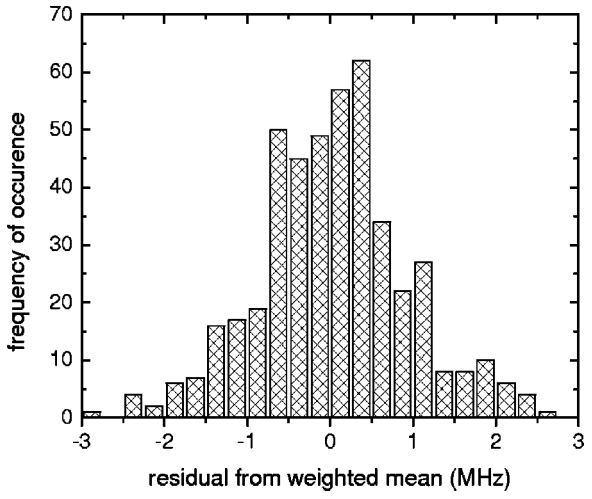

Fig. 4. Residuals for all wave-number measurements calculated by comparison of individual measurements with their weighted means. The standard deviation of the resulting histogram of 457 measurements is 0.97 MHz. This estimate of the measurement reproducibility is the dominant contribution to the final measurement uncertainty.

The shapes of the Doppler-free Te_2 absorptions have been investigated to determine the maximum potential shift of the line center that could result from any asymmetries. Although all measured absorption lines are at first glance symmetric, three stronger lines were randomly chosen for further scrutiny. Their line shapes were repeatedly recorded and analyzed with both a symmetric Lorentzian function and a Lorentzian function with different left and right half-widths. Differences in the frequencies of the line centers for the two fitting functions indicate that, at the present signal-to-noise ratio, 0.2 MHz is an upper limit on any possible shift of the measured line center owing to line-shape asymmetries.

Nonparallelism of the pump and probe beams is a known source of frequency shift in saturation spectroscopy.[39] We estimate our beams to be parallel within 0.67 mrad. For molecules with the most probable speed, this leads to a frequency shift of 0.17 MHz. We include an uncertainty of 0.2 MHz in the error budget.

Assuming that the statistical measurement reproducibility (0.97 MHz) and the uncertainties in the phase correction (0.23 MHz), offset-lock beat frequency (0.20 MHz), pressure shifts (0.30 MHz), line-shape asymmetries (0.20 MHz), and pump-probe parallelism (0.20 MHz) are independent, they were added in quadrature to produce a 1.1-MHz (0.000 037 cm^{-1}) overall uncertainty for the transition wave numbers measured in this work.

5. CONCLUSIONS

We have measured 39 Doppler-free transition wave numbers of $^{130}Te_2$ with an accuracy of better than 2 parts in 10^9 using saturated absorption spectroscopy and FP interferometry. These measurements represent at present the only convenient high-accuracy wavelength standards in the range of 420.9–464.6 nm, spanning the Stilbene 420 dye-tuning curve.

ACKNOWLEDGMENTS

This research was supported by the Canadian Institute for Photonic Innovations, the Natural Sciences and Engineering Research Council of Canada, and by the Academic Development Fund of the University of Western Ontario. We thank Alan Madej of the Institute for National Measurement Standards, National Research Council of Canada, for transferring frequency-offset-locking technology to our laboratory and Craig Sansonetti of the

National Institute of Standards and Technology, Gaithersburg, Maryland, for exchange of ideas and encouraging conversations. We also thank Harry Chen and Doug Hie for technical assistance with the electronics.

REFERENCES

1. G. Guelachvili, "Absolute wavenumber measurements of 1-0, 2-0, HF and 2-0, $H^{35}Cl$, $H^{37}Cl$ absorption bands," Opt. Commun. **19**, 150–154 (1976).
2. S. L. Gilbert, S. M. Etzel, and W. C. Swann, "Wavelength accuracy in WDM: techniques and standards for component characterization," in *Proceedings of Optical Fiber Communication Conference*, Vol. 70 of OSA Trends in Optics and Photonics series (Optical Society of America, Washington, D.C., 2002), pp. 391–393.
3. W. C. Swann and S. L. Gilbert, "Pressure-induced shift and broadening of 1560–1630-nm carbon monoxide wavelength-calibration lines," J. Opt. Soc. Am. B **19**, 2461–2467 (2002).
4. T. Dennis, E. A. Curtis, C. W. Oates, L. Hollberg, and S. L. Gilbert, "Wavelength references for 1300-nm wavelength-division multiplexing," J. Lightwave Technol. **20**, 804–810 (2002).
5. K. Nakagawa, M. de Labachelerie, Y. Awaji, and M. Kourogi, "Accurate optical frequency atlas of the 1.5μm bands of acetylene," J. Opt. Soc. Am. B **13**, 2708–2714 (1996).
6. S. Gerstenkorn and P. Luc, *Atlas du Spectre d'Absorption de la Molécule d'Iode entre 14 800–20 000* cm^{-1} (Editions du Centre National de la Recherche Scientifique, Paris, 1978).
7. S. Gerstenkorn and P. Luc, *Atlas du Spectre d'Absorption de la Molécule d'Iode entre 14 000–15 600* cm^{-1} (Editions du Centre National de la Recherche Scientifique, Paris, 1978).
8. S. Gerstenkorn and P. Luc, *Atlas du Spectre d'Absorption de la Molécule d'Iode entre 19 700–20 035* cm^{-1} (Editions du Centre National de la Recherche Scientifique, Paris, 1983).
9. S. Gerstenkorn, P. Luc, and A. Raynal, *Atlas du Spectre d'Absorption de la Molécule de Brome entre 11 600–19 600* cm^{-1}*, Volume I et II* (Editions du Centre National de la Recherche Scientifique, Paris, 1985).
10. J. Cariou and P. Luc, *Atlas du Spectre d'Absorption de la Molécule de Tellure. 5: 21 100–23 800* cm^{-1} (Editions du Centre National de la Recherche Scientifique, Paris, 1980).
11. J. Cariou and P. Luc, *Atlas du Spectre d'Absorption de la Molécule de Tellure. 2: 18 500–21 200* cm^{-1} (Editions du Centre National de la Recherche Scientifique, Paris, 1980).
12. C. J. Sansonetti, "Precise measurements of hyperfine components in the spectrum of molecular iodine," J. Opt. Soc. Am. B **14**, 1913–1920 (1997).
13. L. Hlousek and W. M. Fairbank, Jr., "High-accuracy wavenumber measurements in molecular iodine," Opt. Lett. **8**, 322-323 (1983).
14. D. Shiner, J. M. Gilligan, B. M. Cook, and W. Lichten, "H_2, D_2, and HD ionization potentials by accurate calibration of several iodine lines," Phys. Rev. A **47**, 4042–4045 (1993).
15. R. Grieser, G. Bönsch, S. Dickopf, G. Huber, R. Klein, P. Merz, A. Nicolaus, and H. Schnatz, "Precision measurement of two iodine lines at 585 nm and 549 nm," Z. Phys. A **342**, 147–150 (1994).
16. S. C. Xu, R. van Dierendonck, W. Hogervorst, and W. Ubachs, "A dense grid of reference iodine lines for optical frequency calibration in the range 595–655 nm," J. Mol. Spectrosc. **201**, 256–266 (2000).
17. B. Bodermann, H. Knöcke, and E. Tiemann, "Widely usable interpolation formulae for hyperfine splittings in the $^{127}I_2$ spectrum," Eur. Phys. J. D **19**, 31–44 (2002), and references therein.
18. T. J. Quinn, "Practical realization of the definition of the metre (1997)," Metrologia **36**, 211–244 (1999).
19. I. Velchev, R. van Dierendonck, W. Hogervorst, and W. Ubachs, "A dense grid of reference iodine lines for optical frequency calibration in the range 571–596 nm," J. Mol. Spectrosc. **187**, 21–27 (1998).
20. B. A. Palmer and R. Engleman, Jr., "Atlas of the thorium spectrum," Los Alamos Scientific Laboratory Rep. LA-9615 (Los Alamos National Laboratory, Los Alamos, N.M., 1983).
21. B. A. Palmer, R. A. Keller, and R. Engleman, Jr., "An atlas of uranium emission intensities in a hollow cathode discharge," Los Alamos Scientific Laboratory Rep. LA-8251-MS (Los Alamos National Laboratory, Los Alamos, N.M., 1980).
22. J. R. M. Barr, J. M. Girkin, A. I. Ferguson, G. P. Barwood, P. Gill, W. R. C. Rowley, and R. C. Thompson, "Interferometric frequency measurements of $^{130}Te_2$ transitions at 486 nm," Opt. Commun. **54**, 217–221 (1985).
23. D. H. McIntyre and T. W. Hänsch, "Absolute calibration to the $^{130}Te_2$ reference line for positronium $1\,^3S_1-2\,^3S_1$ spectroscopy," Phys. Rev. A **34**, 4504–4507 (1986).
24. D. H. McIntyre and T. W. Hänsch, "Interferometric frequency measurement of a $^{130}Te_2$ reference line for muonium 1S-2S spectroscopy," Phys. Rev. A **36**, 4115–4118 (1987).
25. D. H. McIntyre, W. M. Fairbank, Jr., S. A. Lee, T. W. Hänsch, and E. Riis, "Interferometric frequency measurement of $^{130}Te_2$ reference transitions at 486 nm," Phys. Rev. A **41**, 4632–4635 (1990).
26. G. P. Barwood, W. R. C. Rowley, P. Gill, J. L. Flowers, and B. W. Petley, "Interferometric measurements of $^{130}Te_2$ reference frequencies for 1S-2S transitions in hydrogenlike atoms," Phys. Rev. A **43**, 4783–4790 (1991).
27. Ph. Courteille, L. S. Ma, W. Neuhauser, and R. Blatt, "Frequency measurement of $^{130}Te_2$ resonances near 467 nm," Appl. Phys. B Lasers Opt. **59**, 187–193 (1994).
28. P. Cancio and D. Bermejo, "Absolute wavelengths in $^{130}Te_2$: new reference lines for laser spectroscopy coinciding with emissions of the Ar^+ laser," J. Opt. Soc. Am. B **14**, 1305–1311 (1997).
29. J. D. Gillaspy and C. J. Sansonetti, "Absolute wavelength determinations in molecular tellurium: new reference lines for precision laser spectroscopy," J. Opt. Soc. Am. B **8**, 2414–2419 (1991).
30. T. J. Scholl, S. J. Rehse, R. A. Holt, and S. D. Rosner, "A broadband precision wavelength meter based on a scanning Fabry-Pérot interferometer," Rev. Sci. Instrum. **75**, 3318–3326 (2004).
31. C. J. Sansonetti, "Precise laser wavelength measurements: what can we learn from classical spectroscopy?" in *Advances in Laser Science IV*, J. L. Gole, D. F. Heller, M. Lapp, and W. C. Stwalley, eds. (American Institute of Physics, New York, 1988), pp. 548–553.
32. M. S. Sorem and A. L. Schawlow, "Saturation spectroscopy in molecular iodine by intermodulated fluorescence," Opt. Commun. **5**, 148–151 (1972).
33. R. E. Machol and E. R. Westrum, Jr., "Vapor pressure of liquid tellurium," J. Am. Chem. Soc. **80**, 2950–2952 (1958).
34. J. M. Bennett, "Precise method for measuring the absolute phase change on reflection," J. Opt. Soc. Am. **54**, 612–624 (1964).
35. W. Lichten, "Precise wavelength measurements and optical phase shifts. I. General theory," J. Opt. Soc. Am. A **2**, 1869–1876 (1985).
36. K. W. Meissner, "Interference spectroscopy. Part I," J. Opt. Soc. Am. **31**, 405–427 (1941).
37. R. Benoit, "Application des phénomènes d'interférence a des déterminations métrologiques," J. Phys., 3rd Series, **7**, 57–68 (1898).
38. H. Buisson and Ch. Fabry, "Mesures de longueurs d'onde pour l'établissement d'un système de repères spectroscopiques," J. Phys. (Paris) **7**, 169–195 (1908).
39. S. E. Park, H. S. Lee, T. Y. Kwon, and H. Cho, "Dispersion-like signals in velocity-selective saturated-absorption spectroscopy," Opt. Commun. **192**, 49–55 (2001).